APL Photonics

Single-shot isotropic quantitative phase microscopy based on color-multiplexed differential phase contrast

Cite as: APL Photonics 4, 121301 (2019); https://doi.org/10.1063/1.5124535
Submitted: 17 August 2019 . Accepted: 31 October 2019 . Published Online: 03 December 2019

Yao Fan, Jiasong Sun, Qian Chen, Xiangpeng Pan, Maciej Trusiak, and Chao Zuo

openaccess
View Online
Export Citation
CrossMark

AMERICAN ELEMENTS
THE ADVANCED MATERIALS MANUFACTURER®
American Elements opens up a world of possibilities so you can Now Invent!
Over 15,000 certified high purity laboratory chemicals, metals, & advanced materials and a state-of-the-art Research Center. Printable GHS-compliant Safety Data Sheets. Thousands of new products. And much more. All on a secure multi-language "Mobile Responsive" platform.
Now Invent.™
The Next Generation of Material Science Catalogs
www.americanelements.com

© 2019 Author(s).

Single-shot isotropic quantitative phase microscopy based on color-multiplexed differential phase contrast

Cite as: APL Photon. 4, 121301 (2019); doi: 10.1063/1.5124535
Submitted: 17 August 2019 • Accepted: 31 October 2019 •
Published Online: 3 December 2019

View Online Export Citation CrossMark

Yao Fan,[1,2,3,a] Jiasong Sun,[1,2,3] Qian Chen,[1,2,b] Xiangpeng Pan,[1,2,3] Maciej Trusiak,[4] and Chao Zuo[1,2,3,c]

AFFILIATIONS

[1]School of Electronic and Optical Engineering, Nanjing University of Science and Technology, No. 200 Xiaolingwei Street, Nanjing, Jiangsu Province 210094, China
[2]Jiangsu Key Laboratory of Spectral Imaging and Intelligent Sense, Nanjing University of Science and Technology, Nanjing, Jiangsu Province 210094, China
[3]Smart Computational Imaging (SCI) Laboratory, Nanjing University of Science and Technology, Nanjing, Jiangsu Province 210094, China
[4]Warsaw University of Technology, Institute of Micromechanics and Photonics, 8 Sw. A. Boboli St., 02-525 Warsaw, Poland

Note: This paper is part of an APL Photonics Special Topic on Computational Optical Imaging.
[a]**Electronic mail:** fanyaoscilab@163.com
[b]**Electronic mail:** chenqian@njust.edu.cn
[c]**Electronic mail:** zuochao@njust.edu.cn

ABSTRACT

We present a single-shot isotropic quantitative phase imaging method based on color-multiplexed differential phase contrast. In our method, the illumination source is modulated by an LCD into an annular color-multiplexed pattern matching the numerical aperture of the objective precisely to maximize the frequency response for both low and high frequencies (from 0 to $\frac{2NA_{obj}}{\lambda}$). In addition, we propose an alternating illumination scheme to provide a perfectly circularly symmetrical phase transfer function, achieving isotropic imaging resolution and signal-to-noise ratio. A color camera records the light transmitted through the specimen, and three monochromatic intensity images at each color channel are then separated and utilized to recover the phase of the specimen. We display the derivation, implementation, simulation and experimental results, which demonstrate that our method accomplishes high resolution, noise-robustness and reconstruction accuracy phase reconstruction at camera-limited frame rates.

© 2019 Author(s). All article content, except where otherwise noted, is licensed under a Creative Commons Attribution (CC BY) license (http://creativecommons.org/licenses/by/4.0/). https://doi.org/10.1063/1.5124535

Quantitative analysis of 3D structures of living cells at cellular and subcellular levels is highly demanding in biological, biomedical, and pathological research.[1] However, phase contrast (PC) and differential interference contrast (DIC) techniques only provide a qualitative visualization result since the phase of the specimen cannot be directly separated from intensity.[2] Quantitative phase imaging (QPI) provides an invaluable optical tool for living cell research owing to its unique capabilities to image optical thickness variation of living cells and tissues without the need for specific staining or exogenous contrast agents (e.g., dyes or fluorophores).[3–5] In contrast to qualitative imaging methods, QPI approaches, such as holography,[6] transport-of-intensity equation (TIE),[7,8] differential phase contrast (DPC),[9,10] and Fourier ptychographic microscopy (FPM),[11,12] recover the phase of the sample from intensity variation caused by optical path-length change, allowing for various quantitative studies, such as the measurement of cellular mechanical properties and dynamic transport of intracellular structures.[13,14] Among these approaches, DPC is a very promising approach for imaging living cells *in vitro* due to its higher imaging efficiency, reconstruction accuracy, and robustness.[10]

© Author(s) 2019

DPC recovers the quantitative phase of the specimen based on one-step deconvolution of several images and the system's phase transfer function (PTF), achieving a resolution up to the incoherent resolution limit (2× better than the resolution of coherent methods). Typically, the illuminations of DPC are designed with a complementary half-circle pupil with 2-axis (i.e., 4 images) measurements along orthogonal directions.[10,15] However, multiple measurements reduce the temporal resolution of DPC, precluding observation of a high-speed phenomenon. To improve the imaging efficiency, color-multiplexed illumination is adopted in DPC, where the 4 source patterns were encoded into 2 images by using a color camera in combination with a color light-emitting diode (LED) array.[16] Furthermore, some efforts have been made toward developing single-shot DPC mechanisms by using trimode illumination or adding a multicolored filter.[17,18] These methods reduce the number of captured images to a single exposure; however, the frequency responses of the PTFs have not been improved, leading to poor phase contrast and signal-to-noise ratio (SNR) for phase reconstruction. Specifically, the PTF cannot achieve isotropic frequency response and still suffers a weak response at the central low frequency and the high frequency approaching the cutoff frequency of partially coherent imaging $\frac{2NA_{obj}}{\lambda}$ (NA_{obj} is the numerical aperture of the objective, and λ is the illumination wavelength) so that the phase information at the same resolution cannot be completely restored.

In order to optimize the phase imaging quality of single-shot DPC, in this letter, we present a new single-shot illumination scheme based on color-multiplexed illumination for achieving high-resolution, high-accuracy, and high robust isotropic DPC imaging. In our method, the illumination source is modulated by a high contrast LCD into an annular color-multiplexed pattern matching the numerical aperture (NA) of the objective precisely to maximize the frequency response for both low and high frequencies (from 0 to $\frac{2NA_{obj}}{\lambda}$). In addition, we provide an alternating illumination scheme to obtain a perfectly circularly symmetrical PTF, achieving isotropic lateral resolution and SNR.

Considering a pure phase object with transmission function $tra(r) = e^{i\phi(r)} \approx 1 + i\phi(r)$ [weak object approximation, $r = (x, y)$ is the spatial coordinate] is illuminated by an oblique plane wave with intensity distribution $S(u_j)$ (j denotes titled illumination at different angles, and u_j represents the corresponding frequency shift vector induced by the tilted illumination). The intensity spectrum of the bright-field image under oblique illumination can be separated as

$$I_j(u) = S(u_j)\delta(u) + iS(u_j)\Phi(u)\left[P^*(u_j)P(u+u_j) - P(u_j)P^*(u-u_j)\right], \tag{1}$$

where $u = (k_x, k_y)$ is the coordinate at the Fourier space, and $P(u)$ denotes the pupil function of the objective lens (an ideal low-pass filter with a cutoff frequency of $\frac{NA_{obj}}{\lambda}$). Traditional DPC requires a pair of captured images, where each partially coherent illumination function has complementary gradient vector to generate a phase gradient image along a specific direction. We reduce the captured image along a specific direction to one implementation by removing the zero frequency component $\delta(u)$ in Eq. (1), also leaving only the phase gradient term

$$I_l^{DPC}(u) = I_l(u) - B\delta(u) = i\Phi(u)PTF_l(u), \tag{2}$$

where B is the background term and l denotes the angle of the asymmetric axis of the DPC illumination. For example, the asymmetric angle l of traditional left-right illumination DPC can be seen at 0 rad. Thus, the PTF can be denoted as

$$PTF_l(u) = \iint S_l(u_j) \times \left[P^*(u_j)P(u+u_j) - P(u_j)P^*(u-u_j)\right]d^2u_j. \tag{3}$$

Equation (3) shows that once the optical configuration of the microscope is fixed [$P(u)$ is predefined], the PTF is fully determined by the DPC illumination S_l. The sample's quantitative phase is recovered by solving the inverse problem with one-step deconvolution,[19]

$$\phi(r) = \mathscr{F}^{-1}\left\{\frac{\sum_l\left[PTF_l^*(u)\cdot I_l^{DPC}(u)\right]}{\sum_l |PTF_l^*(u)|^2 + \beta}\right\}, \tag{4}$$

where $PTF_l^*(u)$ denotes the complex conjugation of PTF. The Tikhonov regularization parameter β is introduced into Eq. (4) to avoid singularity in PTF inversion.

In order to improve the imaging performance of DPC, we use the polar coordinate system to replace the Cartesian coordinate to separate the effects of radius and angle. Instead of using uniform circle illumination, we propose the optimal illumination scheme for 3-axis DPC to optimize imaging performance, and the illumination functions along three different axes are set as

$$\begin{aligned} S_l(\rho,\theta) &= \delta\left(\rho - \frac{NA_{obj}}{\lambda}\right)sin(\theta + l), \\ l_{1,2,3} &= \frac{-2\pi}{3}, 0, \frac{2\pi}{3}, \qquad (\theta + l) \in (0, \pi], \end{aligned} \tag{5}$$

where ρ and θ represent the radius and the polar angle in the polar coordinate, respectively, and $l_{1,2,3} = -\frac{2\pi}{3}, 0, \frac{2\pi}{3}$ denotes the asymmetry axis of the three illumination patterns. They are evenly distributed in the range of $(-\pi, \pi]$ to avoid the unbalanced PTF response caused by the illumination angle. Different from the previous research of restricting the illumination aperture from being a circle, our illumination is set to be an annulus with the diameter matching the objective pupil and the smallest thickness. In our latest work, it has been proved that this annular illumination could provide the optimal PTF response of an incoherent imaging system.[20,21]

For general illumination, the PTF in a polar coordinate system can be calculated by integrating the overlap of the source and pupil functions, and the specific expression has been derived.[20] Then, the illuminations in Eq. (5) are used to calculate the PTF along the three illumination axes as follows:

$$PTF_l(\rho,\theta) = \sin(\alpha)\sin(\theta + l), \tag{6}$$

where α is determined by $\cos(\alpha) = \frac{\rho\lambda}{2NA_{obj}}$. Generally, the synthetic square of the amplitude of the multiaxial PTFs $[\sum_l |PTF_l^*(\rho,\theta)|^2$, shorten as $K(\rho, \theta)]$ in Eq. (4), is calculated to measure the imaging performance in DPC imaging.[10] In this case, we can further summarize Eq. (6) to calculate $K(\rho, \theta)$ under monochrome illumination,

$$K(\rho,\theta) = \frac{3}{2}\left(1 - \frac{\rho^2\lambda^2}{4NA_{obj}{}^2}\right). \tag{7}$$

© Author(s) 2019

Equation (7) shows that $K(\rho, \theta)$ is only related to ρ, which indicates that Eq. (5) in monochrome illumination produces an isotropic PTF. Since color-multiplexed DPC has more complex illumination functions and pupil functions, Eq. (7) generally has no analytical solution. So the $K(\rho, \theta)$ of our single-shot DPC will be analyzed by numerical simulation in the following.

The optimal 3-axis illumination scheme is used for our single-shot DPC based on color-multiplexed illumination. In our case, the 3-axis illuminations with wavelengths of λ_r, λ_g, and λ_b are turned on simultaneously, recording only one color image. In Fig. 1(a), we show the schematic diagram of the proposed system. An LCD is placed on the front focal plane of the condenser,[22] so the illumination source is modulated into the pattern, as shown in Fig. 1(b-1). Compared to the LED illumination source, the array units of the LCD are sufficiently dense to produce an approximately continuous illumination source, which means more frequency sampling on the Fourier plane. The resulting PTF achieves a broadband frequency coverage for partially coherent imaging (from 0 to $\frac{2NA_{obj}}{\lambda_b}$) with a smooth and significantly enhanced response, as shown in Fig. 1(c-1). Then, a sample image [shown in Fig. 1(d-1)] is recorded by a color camera and is then separated into three monochromatic intensity images corresponding to three channels based on a color cross talk correction algorithm.[23] In the deconvolution process, these three monochromatic images are used to reconstruct the sample's phase according to Eq. (4). It should be noted that the phase changes inversely with the wavelength for the same phase object *i.e.*, $\phi \propto \frac{1}{\lambda}$; thus, we need to normalize these three illuminations to a selected wavelength. In our method, we normalize these three wavelengths to the blue wavelength by multiplying the spectrum of the phase gradient image by a wavelength normalization coefficient $\frac{\lambda_b}{\lambda_c}$ (λ_c is the three illumination wavelength, $c = r, g, b$). Finally, the phase result, as shown in Fig. 1(e-1), can be obtained.

It should also be noted that because the radius of pupil function $P(u)$ is inversely proportional to the illumination wavelength, the spectrum support domains of PTFs vary with wavelengths. Hence, three illumination wavelengths result in uneven coverage of Fourier space. Aiming to obtain a perfectly isotropic PTF, we further propose an alternating illumination scheme. Illumination pattern 1 is rotated by 90° to generate illumination pattern 2 [Fig. 1(b-2)], and these two patterns illuminate the sample alternately. This alternating illumination yields isotropic $K(\rho, \theta)$ on each color channel, resulting in an isotropic $K(\rho, \theta)$ in color-multiplexed illumination. For slow-moving samples, each frame and its adjacent frame can be used to recover the phase with isotropic resolution and SNR at camera-limited frame rates, achieving high quality single-shot QPI.

In order to verify the imaging performance of our method, we simulated $K(\rho, \theta)$ for different single-shot DPC methods, as shown in Fig. 2. As shown in 2(a-1), 2(a-2), 2(b-1), and 2(b-2), the PTF under trimode and sine circle illumination has very low response at both low and high frequencies, which indicates poor SNR and poor resolution of the phase reconstruction. Our sine annular illumination significantly enhances the responses of $K(\rho, \theta)$ at almost all frequencies of the entire partially coherent imaging (from 0 to $\frac{2NA_{obj}}{\lambda_b}$) [Figs. 2(a-3) and 2(b-3)] and even achieves a perfectly isotropic $K(\rho, \theta)$. To further compare our method's difference of PTF response with other illuminations, we show the PTF difference between our sine annular illumination and trimode and sine circle illuminations in 2(c-1), 2(c-2), 2(d-1), and 2(d-2) [subtract the PTF of Figs. 2(a-1) and 2(a-2) from the PTF of Fig. 2(a-3), respectively]. It can be seen more clearly that the amplitudes of $K(\rho, \theta)$ under

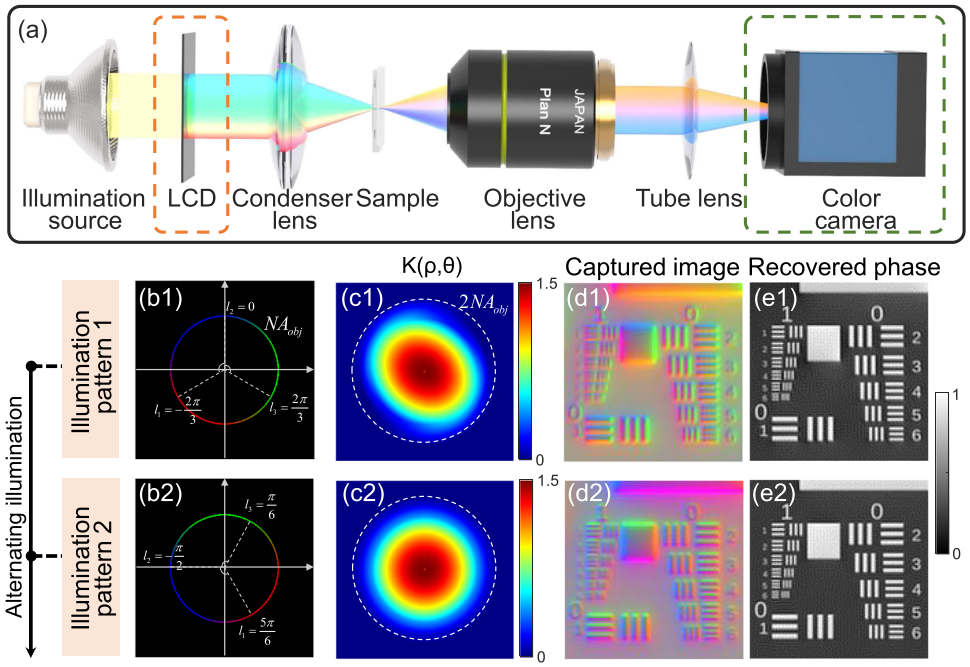

FIG. 1. The schematic diagram of our proposed method. (a) The schematic of the imaging system. [(b1) and (b2)] Illumination patterns. [(c1) and (c2)] $K(\rho, \theta)$ under the illumination patterns (b1) and (b2). [(d1) and (d2)] Captured images. [(e1) and (e2)] Recovered phases.

© Author(s) 2019

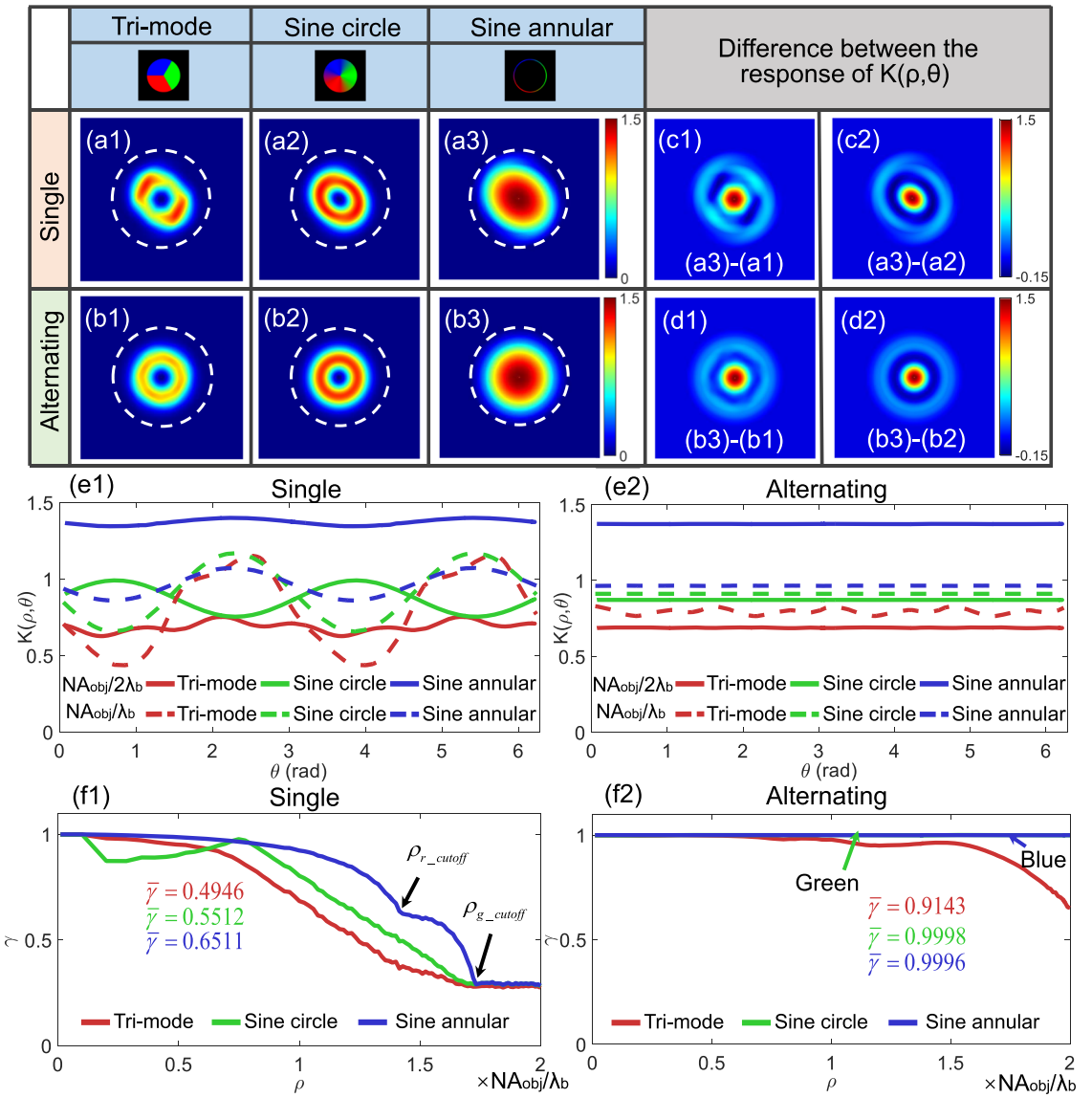

FIG. 2. Simulation of different DPC illumination patterns. [(a-1)–(a-3)] $K(\rho, \theta)$ under different single-shot DPC illumination patterns. [(b-1)–(b-3)] $K(\rho, \theta)$ under different alternating illumination patterns. [(c-1), (c-2), (d-1), and (d-2)] Difference between the response of $K(\rho, \theta)$. [(e-1) and (e-2)] Quantitative curves of $K(\rho, \theta)$ on $NA_{obj}/2\lambda_b$ and NA_{obj}/λ_b under single and alternating illumination. [(f-1) and (f-2)] Quantitative curves of $\gamma(\rho)$ under single and alternating illumination.

our illumination obviously enhance at the low frequency near the zero frequency and the high frequency approaching $\frac{NA_{obj}}{2\lambda_b}$, which not only alleviates the ill-posedness of the PTF inversion but also ensures higher phase contrast. To quantitatively compare the isotropy of these illuminations, the response values on $\frac{NA_{obj}}{2\lambda_b}$ and $\frac{NA_{obj}}{\lambda_b}$ of $K(\rho, \theta)$ are extracted to plot curves, as shown in Figs. 2(e-1) and 2(e-2). Obviously, our single and alternating illuminations (blue lines) always achieve a most stable response at each radius. We introduce an isotropy evaluation coefficient $\gamma(\rho)$ to quantify the degree of isotropy, which calculates the ratio of the standard deviation to the mean of the $K(\rho, \theta)$ response at a different radius ρ to characterize the isotropy of different frequency components,

$$\gamma(\rho) = 1 - \frac{std[K(\rho,\theta)]}{mean[K(\rho,\theta)]}. \tag{8}$$

A stable $\gamma(\rho)$ equal to 1 means that $K(\rho, \theta)$ is completely isotropic, and the value of $\gamma(\rho)$ decreases when anisotropy appears. Then, the mean value $\bar{\gamma}$ is solved to quantitatively evaluate the overall isotropy of $K(\rho, \theta)$. Figures 2(f-1) and 2(f-2) show the $\gamma(\rho)$ numerical curves and $\bar{\gamma}$ under these illuminations. Figures 2(f-1) show that our single

© Author(s) 2019

illumination significantly increases the $\gamma(\rho)$ value within the green cutoff frequency ρ_{g_cutoff} ($\rho_{g_cutoff} = \frac{2NA_{obj}}{\lambda_g}$), and a $\overline{\gamma}$ closer to 1 can be obtained, indicating that it enhances the isotropy of the single-shot DPC imaging. Meanwhile, a $\overline{\gamma}$ approaching 1 is obtained under our alternating illumination [Fig. 2(f-2)], proving that it achieves complete isotropy from 0 to $\frac{2NA_{obj}}{\lambda_b}$.

We compare the proposed single and alternating illumination DPC with the trimode DPC experimentally using a phase

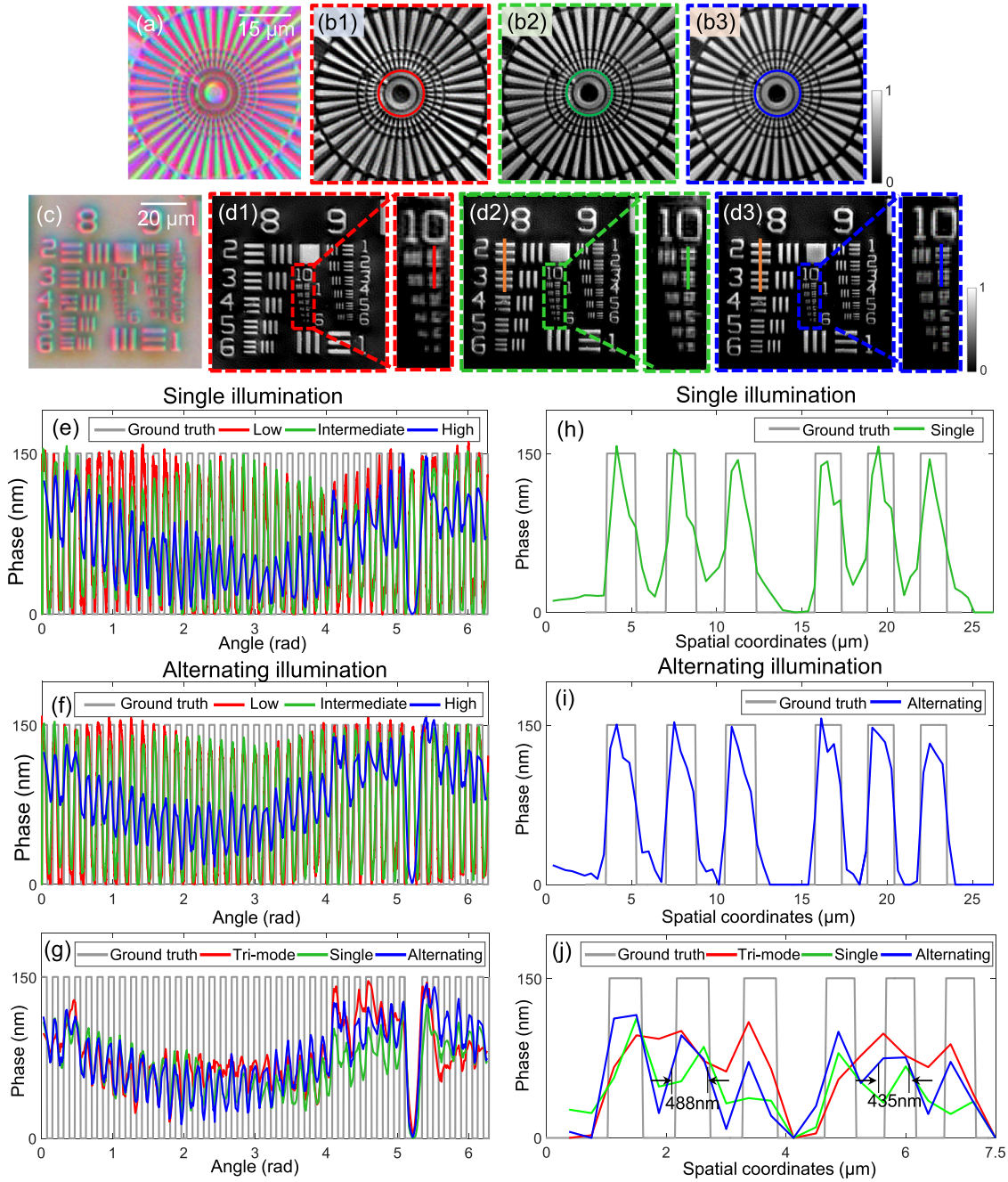

FIG. 3. Experimental results of the phase resolution target *QPT*^{TM}. [(a) and (c)] Captured color images of our single-shot method. [(b-1)–(b-3) and (d-1)–(d-3)] Recovered phase results under trimode illumination, single illumination, and alternating illumination. [(e) and (f)] Phase values along small circles of low frequency, intermediate frequency, and high frequency under our single illumination and alternating illumination. (g) Phase values along the red, green, and blue circles of the same radius (highest frequency) in (b-1)–(b-3). [(h) and (i)] Phase values along the yellow lines in (d-2) and (d-3). (g) Phase values along the red, green and blue lines (highest frequency) in (d-1)–(d-3).

© Author(s) 2019

resolution target [quantitative phase microscopy target (QPT^{TM}), Benchmark Technologies Corporation, U.S.]. Our setup was built based on an inverted microscope (IX83, Olympus), in which a high contrast amorphous Silicon (a-Si) thin film transistor (TFT) LCD screen (4.3 in., 480 × 272) is controlled by computer software via universal serial bus (USB) with an STM32 microcontroller to generate the illumination with wavelengths of 461, 517, and 630 nm. The extinction ratio of this LCD is 600:1 with use of a simple "full on/full off" method. The illumination source modulated by this LCD has sufficient intensity to capture images at camera-limited frame rates. The images are captured by an objective lens with a magnification of 10× and a NA of 0.25 (Olympus PLAN) and finally digitalized by a color CCD camera with a pixel size of 3.75 μm (the imaging source DFK 23U445). In Fig. 3(a), we show the captured color image by our single illumination, and the results under trimode illumination, single illumination, and alternating illumination are shown in Figs. 3(b-1)–3(b-3). It can be seen that, compared with trimode illumination [Fig. 3(b-1)], our single and alternating illuminations significantly improve the resolution and robustness of the phase results. To quantify the resolution and SNR of the reconstructed phase, the line profiles along small circles of different frequencies of Figs. 3(b-2) and 3(b-3) are extracted to plot curves, as shown in Figs. 3(e) and 3(f). Obviously, the phase resolution at all frequencies can be clearly resolved, which means that our single and alternating illuminations achieve isotropic resolution. In addition, the reconstructed phase has stable phase contrast that is consistent with the ground truth phase (150 nm) at almost all frequencies, meaning that it achieves isotropic SNR. We further extract the phase values along a small circle of highest frequency (the theoretical highest resolution being 461 nm) and plot their quantitative curves, as shown in Fig. 3(g). It can be seen that the trimode illumination cannot restore detailed information correctly, yet our single and alternating illuminations achieve isotropic resolution. An additional experiment on the standard resolution QPI target was conducted to demonstrate the achievable highest resolution. We extract the phase values of the yellow lines, as shown in Figs. 3(d-2) and 3(d-3), to plot the quantified curves, as shown in Figs. 3(h)–3(j). Our illumination achieves a consistent result with the ground truth phase for different resolution targets. Furthermore, Fig. 3(j) shows that the smallest differentiable unit (Group 10 Element 2), which corresponds to a half-pitch resolution about 435 nm, can be clearly recovered.

Since our single-shot DPC recovers high resolution phase images within only a single exposure, it can be served as an imaging tool for the visualization and the quantity analysis of the morphology of living cells. As shown in Fig. 4 (Multimedia view), the experiment on unstained Hela cells *in vitro* across 1.65 h was conducted to demonstrate imaging effectiveness at high speed. Figure 4(a) (Multimedia view) shows an example frame from a reconstructed phase video with a video acquisition speed of 30 Hz (see Visualization 1). Two selected zoom-ins of the phase images are shown in Fig. 4(b) (Multimedia view) and Fig. 4(c) (Multimedia view) to observe the subcellular structure in a dynamic process. As shown in Fig. 4(d) (Multimedia view), we further selected a small area [the green-boxed area shown in Fig. 4(a) (Multimedia view)] to study its morphological changes. As we have seen, subcellular dynamics of Hela cell, such as moving vesicles, and shrinking lamellipodium can be clearly observed without any motion-induced blurring or artifacts.

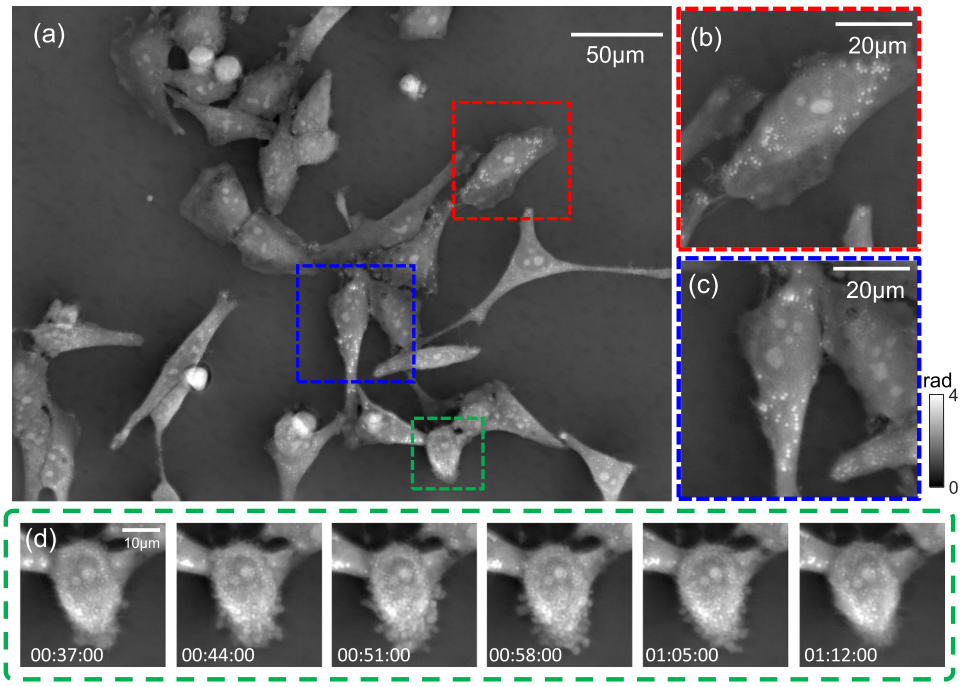

FIG. 4. Phase reconstruction results of Hela cells *in vitro* across 1.65 h. (a) Full field of the view recovered phase. [(b) and (c)] Phase of the two selected zoom-ins. (d) Recovered phase results at different moments. Multimedia view: https://doi.org/10.1063/1.5124535.1

© Author(s) 2019

In conclusion, we proposed a new single-shot isotropic DPC illumination scheme based on color-multiplexed illumination to accomplish high-resolution, high-accuracy, and high-robustness phase retrieval with isotropic lateral resolution and SNR. Compared with the existing single-shot DPC method, our single-shot illumination maximizes the frequency response, which removes the ill-posedness of the PTF inversion so that artifacts in phase reconstruction results can be significantly reduced. Furthermore, an alternating illumination scheme is proposed to produce a perfectly circularly symmetrical PTF, achieving isotropic DPC at camera-limited frame rates. The theoretical analysis, simulations, and experimental results have verified the superiority of our method over other state-of-the-art methods in both phase reconstruction efficiency and accuracy. The experimental results on living Hela cells suggest that our single-shot DPC is a powerful QPI technique for various label-free quantitative living cell imaging, such as drug discovery, cellular phenotype characterization, and identification of disease mechanisms.

This study was supported by the National Natural Science Fund of China (Grant Nos. 61722506, 61505081, and 11574152), the Final Assembly "13th Five-Year Plan" Advanced Research Project of China (Grant No. 30102070102), the Equipment Advanced Research Fund of China (Grant No. 61404150202), the National Defense Science and Technology Foundation of China (Grant No. 0106173), the Outstanding Youth Foundation of Jiangsu Province of China (Grant No. BK20170034), the Key Research and Development Program of Jiangsu Province, China (Grant No. BE2017162), the "Six Talent Peaks" Project of Jiangsu Province, China (Grant No. 2015-DZXX-009), the "333 Engineering" Research Project of Jiangsu Province, China (Grant No. BRA2016407), Fundamental Research Funds for the Central Universities (Grant Nos. 30917011204 and 30916011322), the National Science Centre, Poland (Grant No. 2017/25/B/ST7/02049), the Polish National Agency for Academic Exchange, and the statutory funds of WUT, Fundamental Research Funds for the Central Universities, the Open Research Fund in 2018 of Jiangsu Key Laboratory of Spectral Imaging&Intelligent Sense (Grant No. 3091801410403).

REFERENCES

[1]G. Popescu, *Quantitative Phase Imaging of Cells and Tissues* (McGraw Hill Professional, 2011).
[2]F. Zernike, "Phase contrast, a new method for the microscopic observation of transparent objects part II," Physica **9**, 974–986 (1942).
[3]A. Barty, K. Nugent, D. Paganin, and A. Roberts, "Quantitative optical phase microscopy," Opt. Lett. **23**, 817–819 (1998).
[4]E. Cuche, F. Bevilacqua, and C. Depeursinge, "Digital holography for quantitative phase-contrast imaging," Opt. Lett. **24**, 291–293 (1999).
[5]G. Popescu, "Quantitative phase imaging of nanoscale cell structure and dynamics," Methods Cell Biol. **90**, 87–115 (2008).
[6]P. Marquet, B. Rappaz, P. J. Magistretti, E. Cuche, Y. Emery, T. Colomb, and C. Depeursinge, "Digital holographic microscopy: A noninvasive contrast imaging technique allowing quantitative visualization of living cells with subwavelength axial accuracy," Opt. Lett. **30**, 468–470 (2005).
[7]M. R. Teague, "Deterministic phase retrieval: A Green's function solution," J. Opt. Soc. Am. **73**, 1434–1441 (1983).
[8]C. Zuo, Q. Chen, W. Qu, and A. Asundi, "High-speed transport-of-intensity phase microscopy with an electrically tunable lens," Opt. Express **21**, 24060–24075 (2013).
[9]D. Hamilton and C. Sheppard, "Differential phase contrast in scanning optical microscopy," J. Microsc. **133**, 27–39 (1984).
[10]L. Tian and L. Waller, "Quantitative differential phase contrast imaging in an LED array microscope," Opt. Express **23**, 11394–11403 (2015).
[11]G. Zheng, R. Horstmeyer, and C. Yang, "Wide-field, high-resolution Fourier ptychographic microscopy," Nat. Photonics **7**, 739 (2013).
[12]J. Sun, C. Zuo, L. Zhang, and Q. Chen, "Resolution-enhanced Fourier ptychographic microscopy based on high-numerical-aperture illuminations," Sci. Rep. **7**, 1187 (2017).
[13]B. Bhaduri, C. Edwards, H. Pham, R. Zhou, T. H. Nguyen, L. L. Goddard, and G. Popescu, "Diffraction phase microscopy: Principles and applications in materials and life sciences," Adv. Opt. Photonics **6**, 57–119 (2014).
[14]F. Merola, P. Memmolo, L. Miccio, V. Bianco, M. Paturzo, and P. Ferraro, "Diagnostic tools for lab-on-chip applications based on coherent imaging microscopy," Proc. IEEE **103**, 192–204 (2015).
[15]L. Tian, J. Wang, and L. Waller, "3D differential phase-contrast microscopy with computational illumination using an LED array," Opt. Lett. **39**, 1326–1329 (2014).
[16]D. Lee, S. Ryu, U. Kim, D. Jung, and C. Joo, "Color-coded LED microscopy for multi-contrast and quantitative phase-gradient imaging," Biomed. Opt. Express **6**, 4912–4922 (2015).
[17]Z. F. Phillips, M. Chen, and L. Waller, "Single-shot quantitative phase microscopy with color-multiplexed differential phase contrast (cDPC)," PLoS One **12**, e0171228 (2017).
[18]W. Lee, D. Jung, S. Ryu, and C. Joo, "Single-exposure quantitative phase imaging in color-coded LED microscopy," Opt. Express **25**, 8398–8411 (2017).
[19]M. Bertero and P. Boccacci, *Introduction to Inverse Problems in Imaging* (CRC Press, 1998).
[20]Y. Fan, J. Sun, Q. Chen, X. Pan, L. Tian, and C. Zuo, "Optimal illumination scheme for isotropic quantitative differential phase contrast microscopy," Photonics Res. **7**, 890–904 (2019).
[21]C. Zuo, J. Sun, J. Li, J. Zhang, A. Asundi, and Q. Chen, "High-resolution transport-of-intensity quantitative phase microscopy with annular illumination," Sci. Rep. **7**, 7654 (2017).
[22]K. Guo, Z. Bian, S. Dong, P. Nanda, Y. M. Wang, and G. Zheng, "Microscopy illumination engineering using a low-cost liquid crystal display," Biomed. Opt. Express **6**, 574–579 (2015).
[23]Y. Wu, Y. Zhang, W. Luo, and A. Ozcan, "Demosaiced pixel super-resolution for multiplexed holographic color imaging," Sci. Rep. **6**, 28601 (2016).

© Author(s) 2019